Response of a Zn(II)-based Metal-Organic Coordination Polymer towards Trivalent Metal Ions (Al^{3+}, Fe^{3+}, Cr^{3+}) Probed by Spectroscopic Approaches

Pooja Daga,[a] Priyanka Manna,[b] Prakash Majee,[a] Debal Kanti Singha,[a,b] Sayani Hui,[b] Ananta Kumar Ghosh,[c] Partha Mahata[b*] and Sudip Kumar Mondal[a*]

[a]Department of Chemistry, Siksha-Bhavana, Visva-Bharati University, Santiniketan-731235, West Bengal, India. Email: sudip.mondal@visva-bharati.ac.in

[b]Department of Chemistry, Jadavpur University, Jadavpur, Kolkata-700 032, West Bengal, India.

Email: parthachem@gmail.com

[c]Department of Chemistry, Burdwan Raj College, Burdwan, Burdwan-713104, West Bengal, India

ELECTRONIC SUPPLEMENTARY INFORMATION

* Corresponding Authors, E-mail: sudip.mondal@visva-bharati.ac.in, parthachem@gmail.com

Table S1. Selected bond distances (Å) observed in [Zn(5-AIP)(Ald-4)]·H_2O, **1**

Bond	Distances, Å	Bond	Distances, Å
Zn(1)-O(2)	1.945(2)	Zn(1)-N(1)	2.047(3)
Zn(1)-O(3)#1	1.982(2)	Zn(1)-N(3)#2	2.099(3)

Symmetry transformations used to generate equivalent atoms: #1 x,-y+5/2,z-1/2 #2 x,-y+3/2,z-1/2

Table S2. Selected bond angles observed in [Zn(5-AIP)(Ald-4)]·H_2O, **1**

Angle	Amplitude (º)	Angle	Amplitude (º)
O(2)-Zn(1)-O(3)#1	101.33(10)	O(2)-Zn(1)-N(3)#2	110.39(11)
O(2)-Zn(1)-N(1)	105.22(12)	O(3)#1-Zn(1)-N(3)#2	103.36(11)
O(3)#1-Zn(1)-N(1)	132.26(12)	N(1)-Zn(1)-N(3)#2	103.49(11)

Symmetry transformations used to generate equivalent atoms: #1 x,-y+5/2,z-1/2 #2 x,-y+3/2,z-1/2

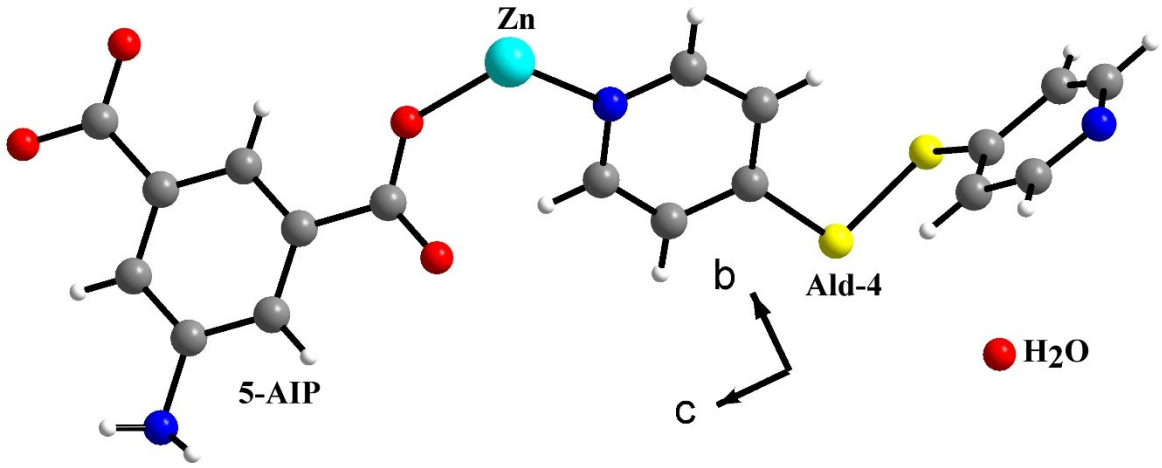

Fig. S1 Figure shows asymmetric unit in the structure of [Zn(5-AIP)(Ald-4)]·H_2O, **1.**

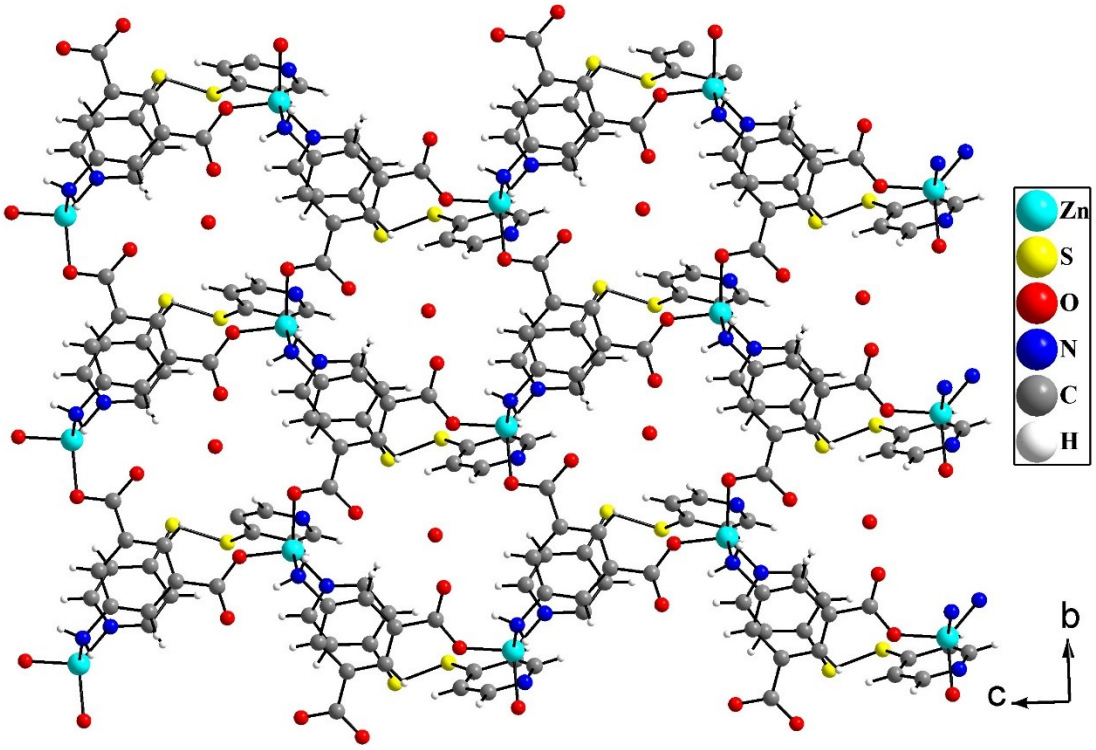

Fig. S2 Figure shows two-dimensional connectivity between Zn^{2+} ions and 5-AIP ligands in *bc* plane along with pendant Ald-4 ligands in $[Zn(5\text{-AIP})(Ald\text{-}4)]\cdot H_2O$, **1.**

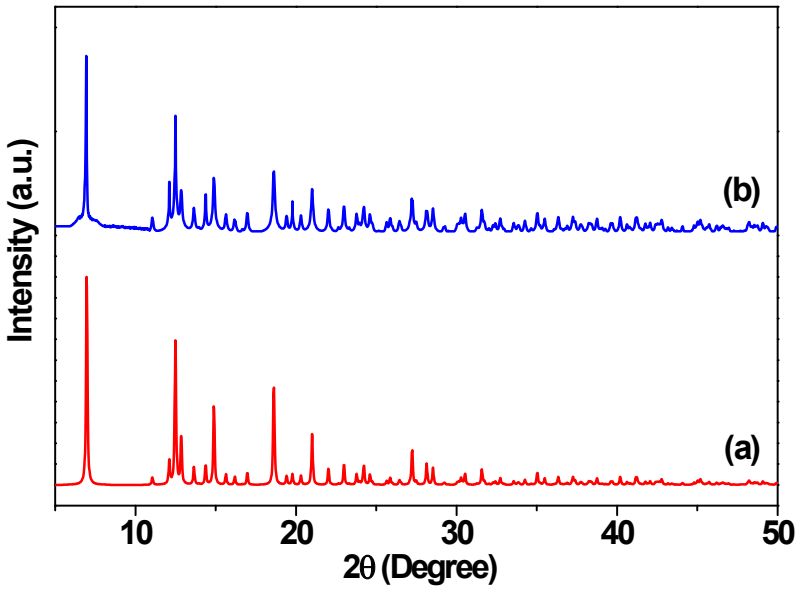

Fig. S3 Powder XRD (Cu Kα) patterns of **1**: (a) simulated from single-crystal X-ray data, (b) experimental.

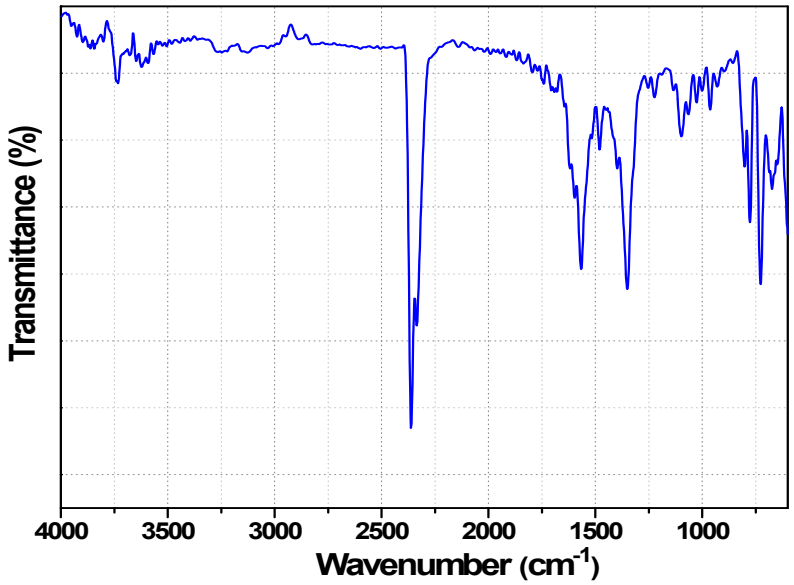

Fig. S4 FTIR spectrum of **1.**

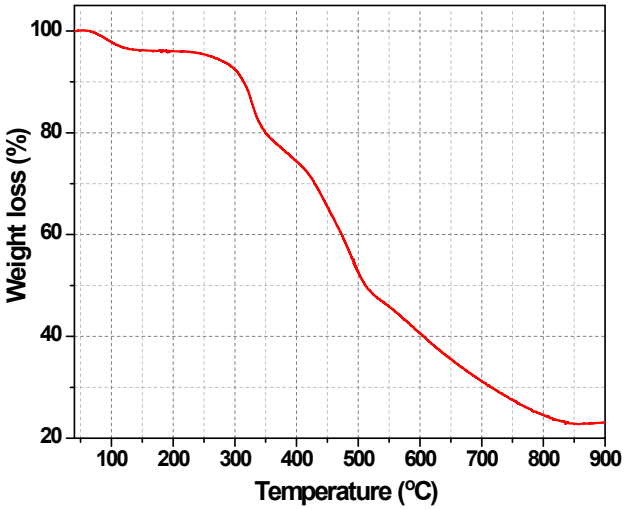

Fig. S5 Thermogravimetric analysis (TGA) data of **1** in a nitrogen atmosphere. The plot shows % weight loss of **1** with the increase in temperature.

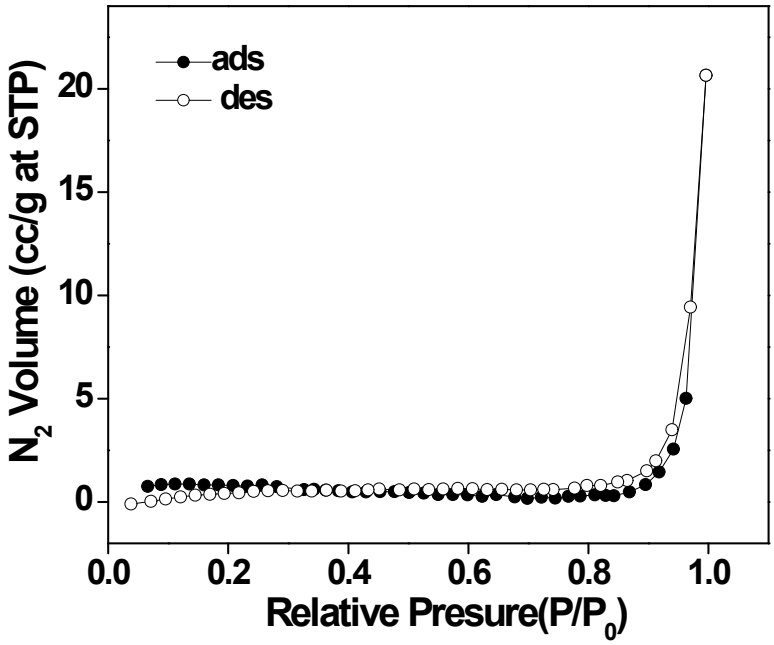

Fig. S6 N_2 sorption isotherm of **1.**

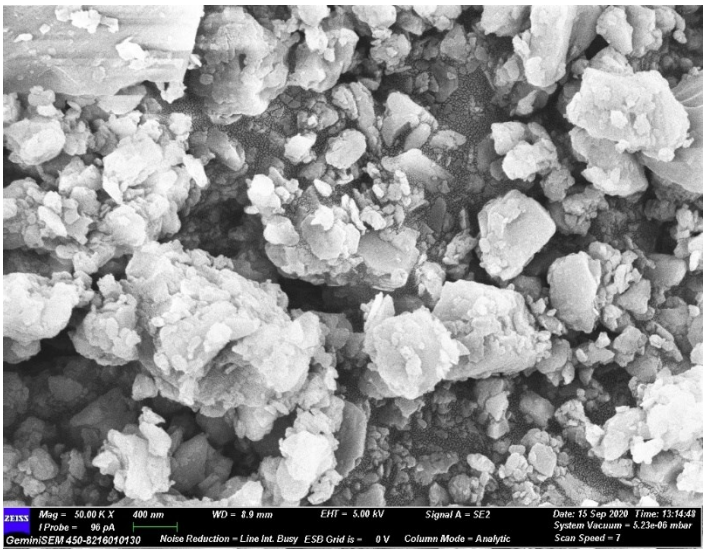

Fig. S7 SEM image of **1**.

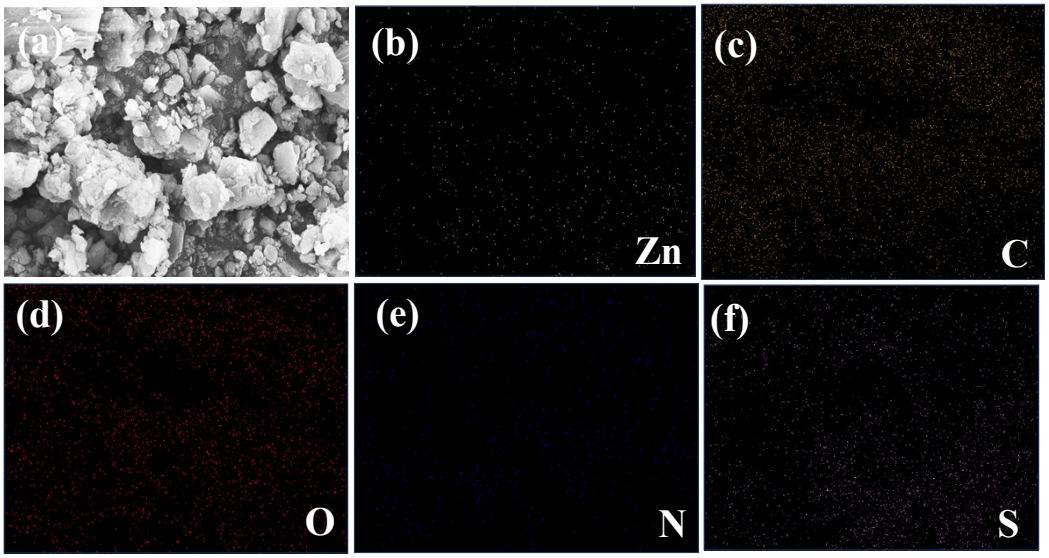

Fig. S8 SEM image in which elemental mapping is performed in **1** and elemental mapping images, (b) Zn K, (c) C K, (d) O K (e) N K and (f) S K.

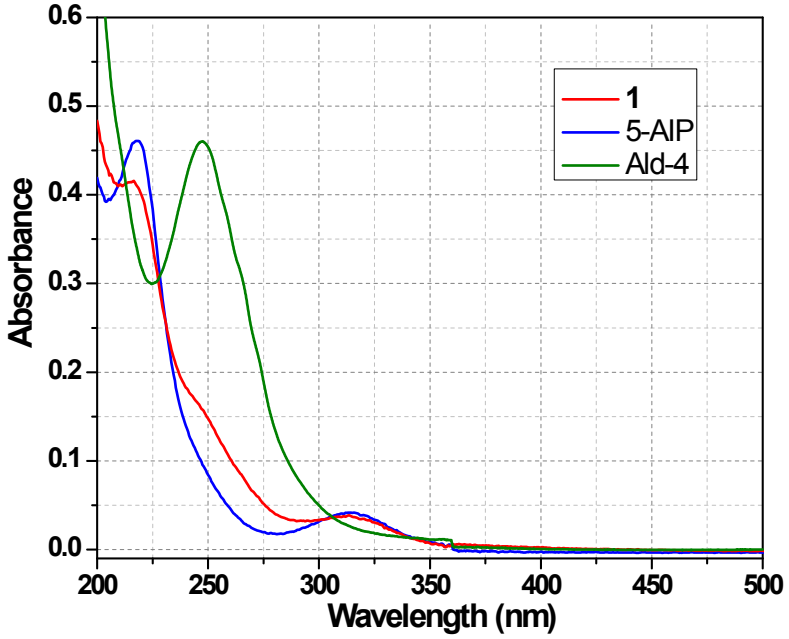

Fig. S9 UV-Visible absorption spectra of **1**, 5-AIP and Ald-4.

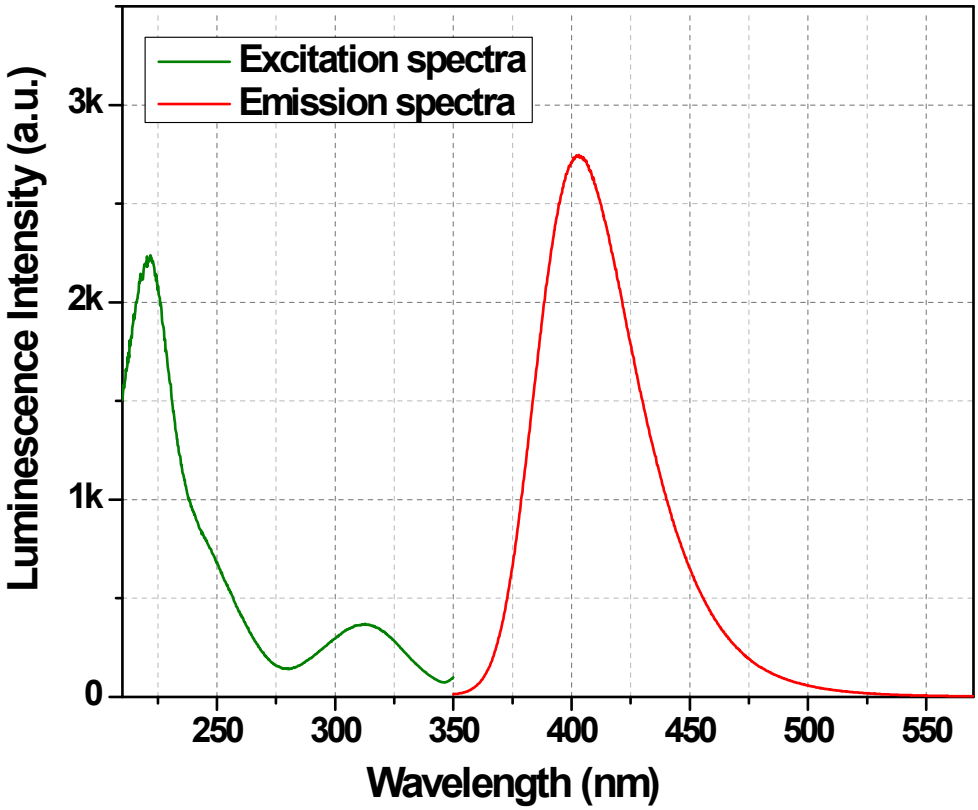

Fig. S10 Excitation and emission spectra of **1**. The excitation wavelength was chosen at 300 nm for emission spectra and for the excitation spectra, emission was fixed at 403 nm.

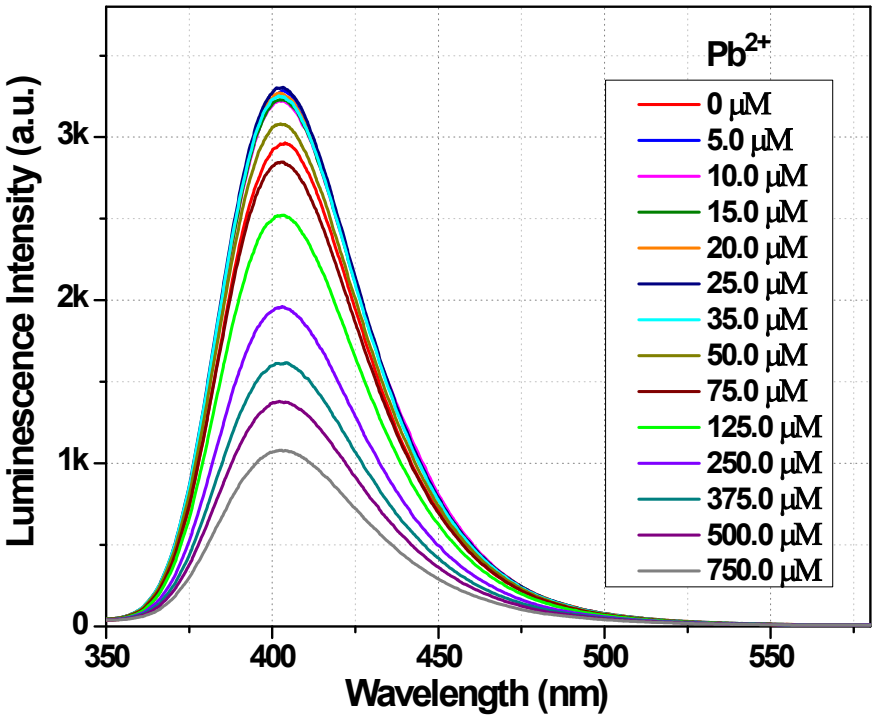

Fig. S11 Emission spectra of **1** dispersed in water upon incremental addition of Pb^{2+} solution (λ_{ex} = 300 nm). The final concentration of Pb^{2+} in the medium is indicated in the legend.

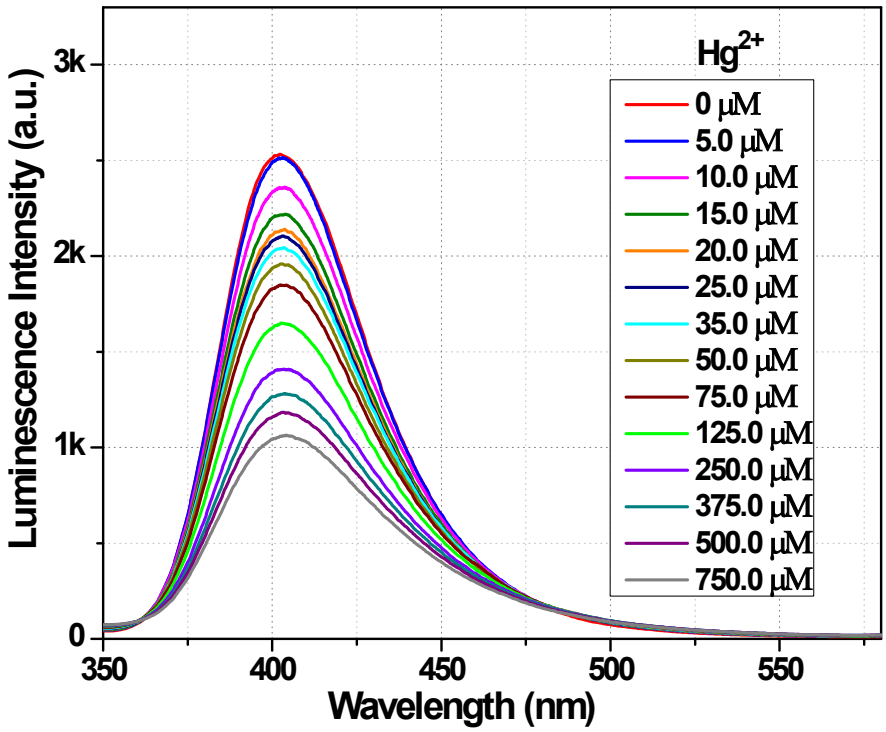

Fig. S12 Emission spectra of **1** dispersed in water upon incremental addition of Hg^{2+} solution (λ_{ex} = 300 nm). The final concentration of Hg^{2+} in the medium is indicated in the legend.

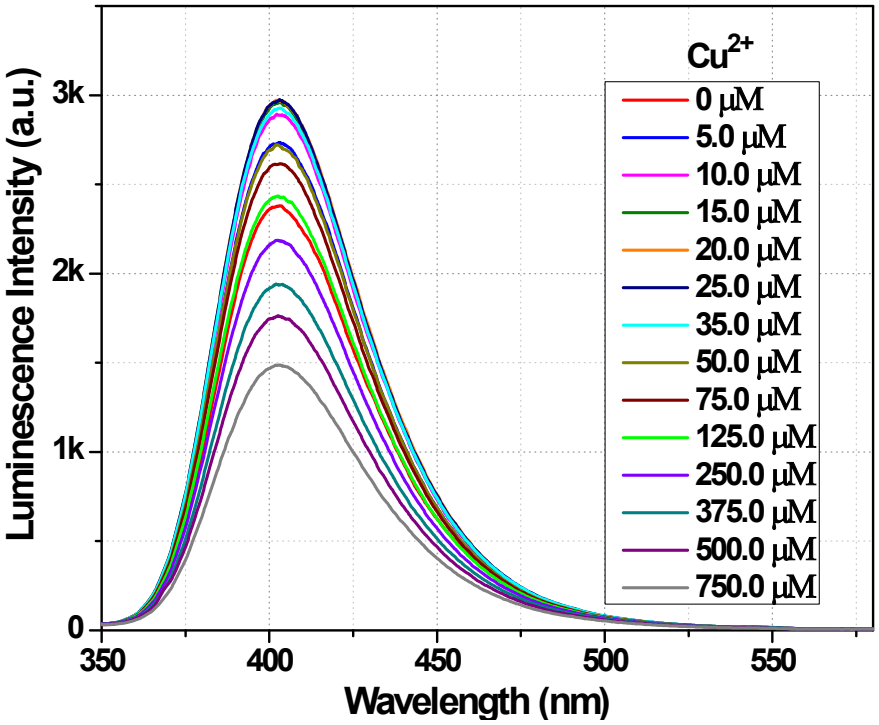

Fig. S13 Emission spectra of **1** dispersed in water upon incremental addition of Cu^{2+} solution (λ_{ex} = 300 nm). The final concentration of Cu^{2+} in the medium is indicated in the legend.

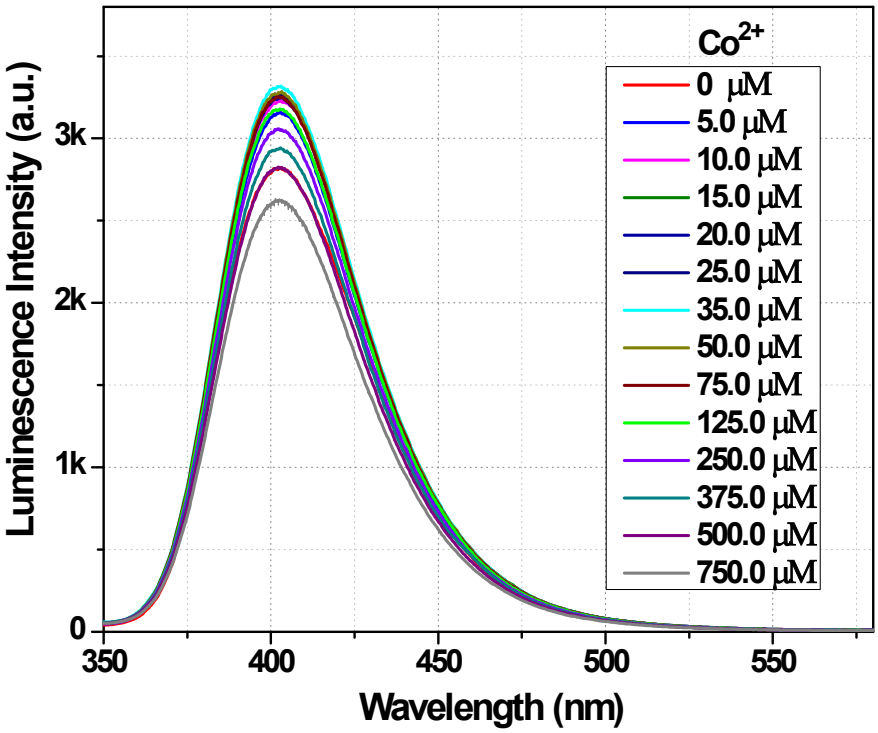

Fig. S14 Emission spectra of **1** dispersed in water upon incremental addition of Co^{2+} solution (λ_{ex} = 300 nm). The final concentration of Co^{2+} in the medium is indicated in the legend.

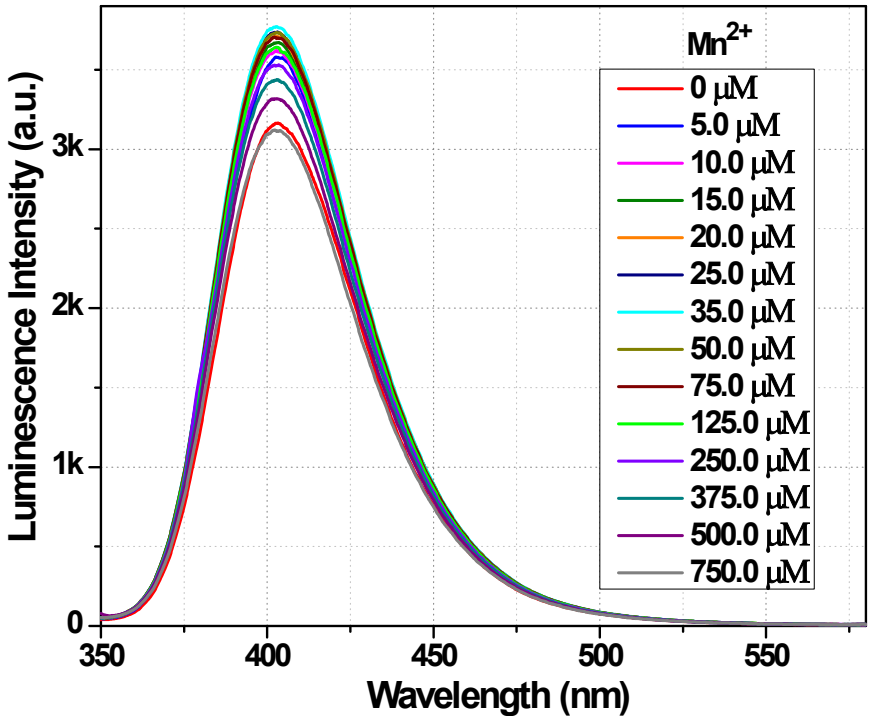

Fig. S15 Emission spectra of **1** dispersed in water upon incremental addition of Mn^{2+} solution (λ_{ex} = 300 nm). The final concentration of Mn^{2+} in the medium is indicated in the legend.

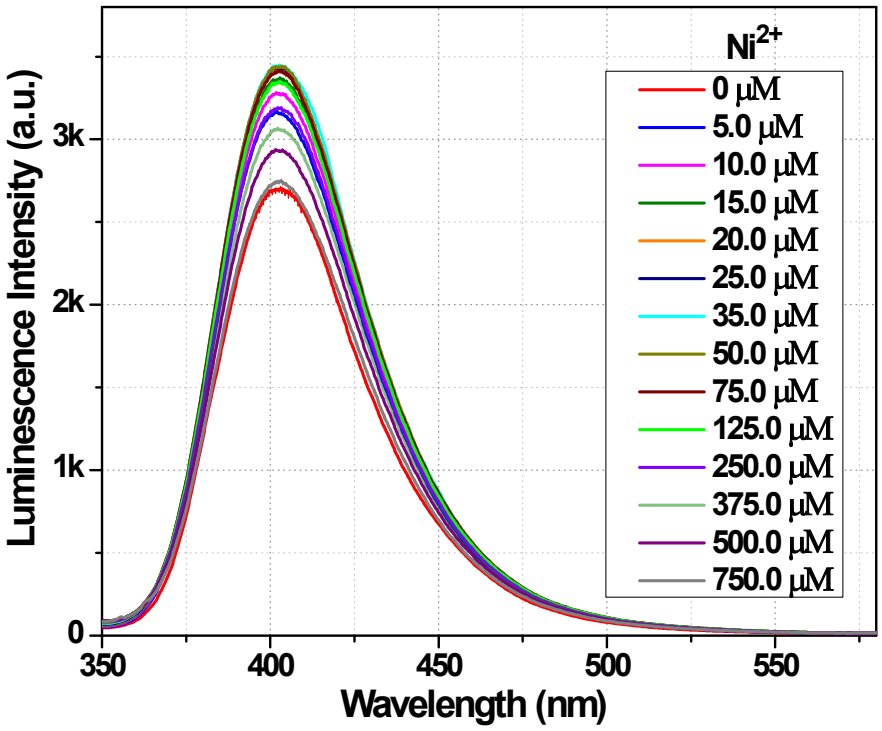

Fig. S16 Emission spectra of **1** dispersed in water upon incremental addition of Ni^{2+} solution (λ_{ex} = 300 nm). The final concentration of Ni^{2+} in the medium is indicated in the legend.

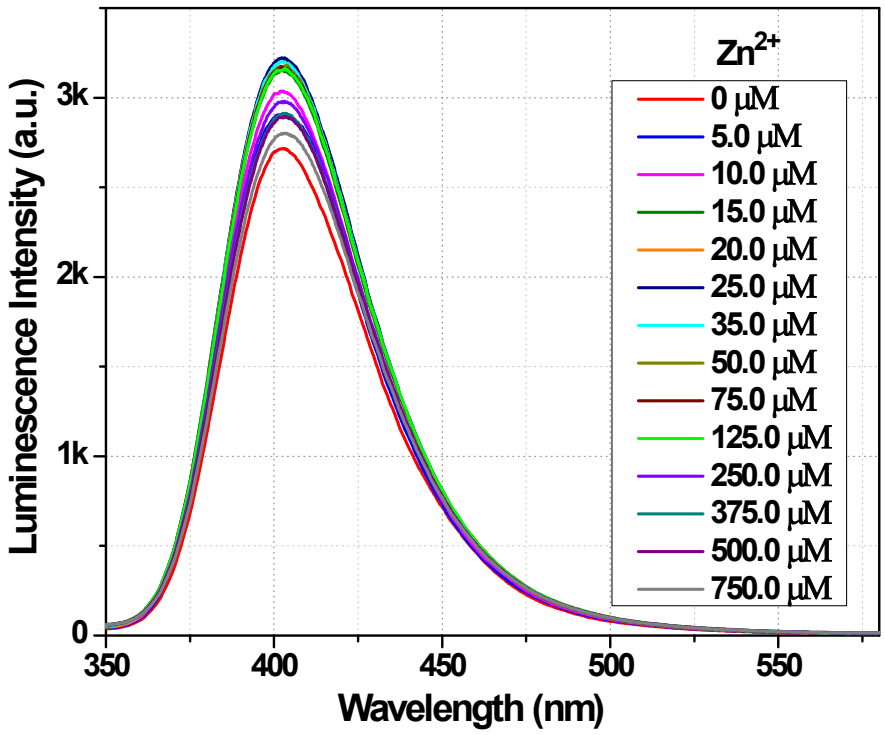

Fig. S17 Emission spectra of **1** dispersed in water upon incremental addition of Zn^{2+} solution (λ_{ex} = 300 nm). The final concentration of Zn^{2+} in the medium is indicated in the legend.

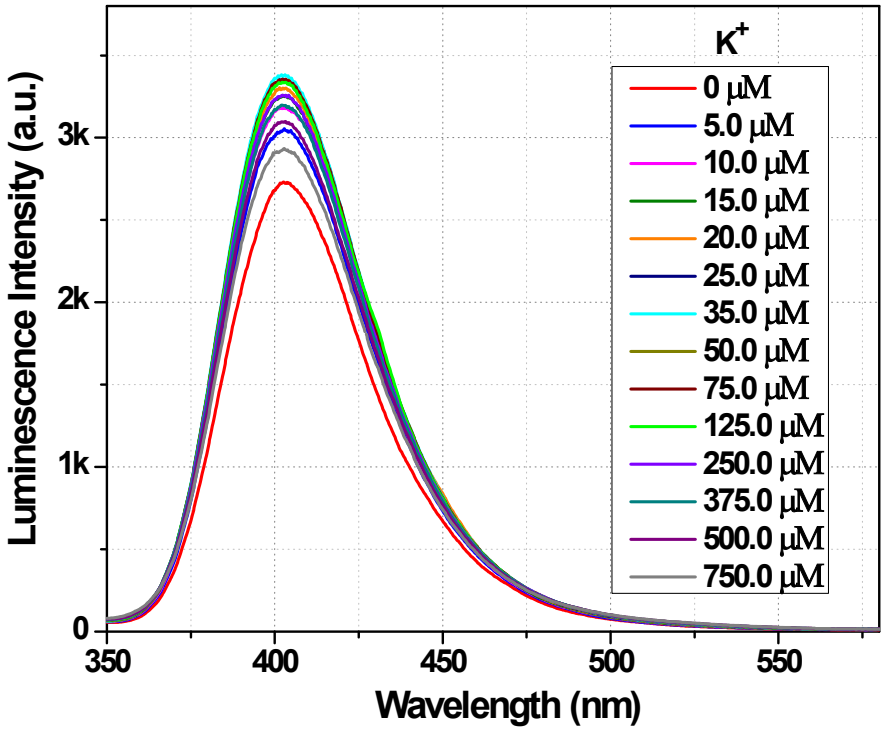

Fig. S18 Emission spectra of **1** dispersed in water upon incremental addition of K^+ solution (λ_{ex} = 300 nm). The final concentration of K^+ in the medium is indicated in the legend.

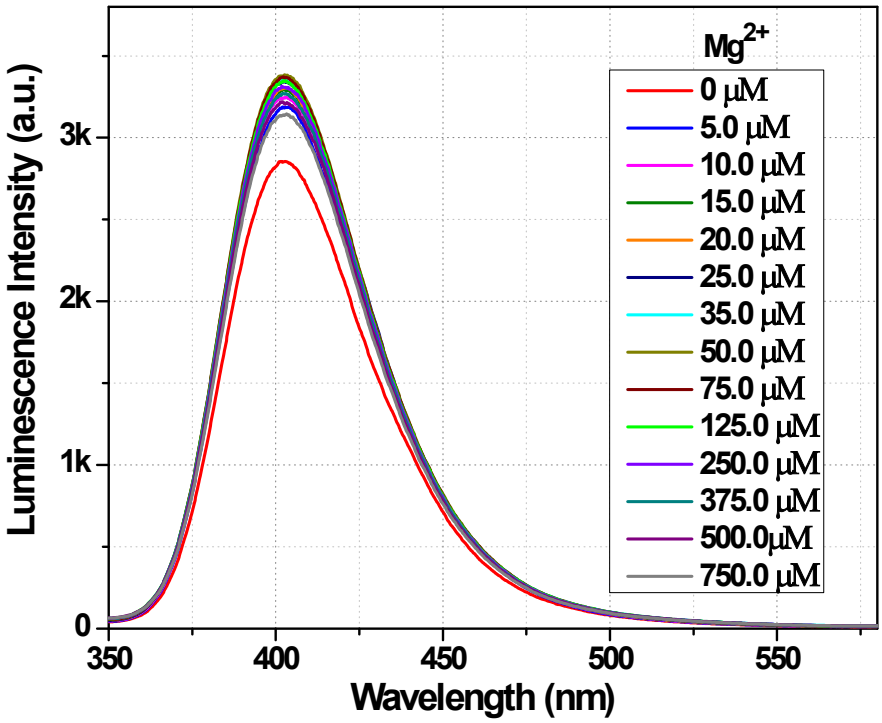

Fig. S19 Emission spectra of **1** dispersed in water upon incremental addition of Mg^{2+} solution (λ_{ex} = 300 nm). The final concentration of Mg^{2+} in the medium is indicated in the legend.

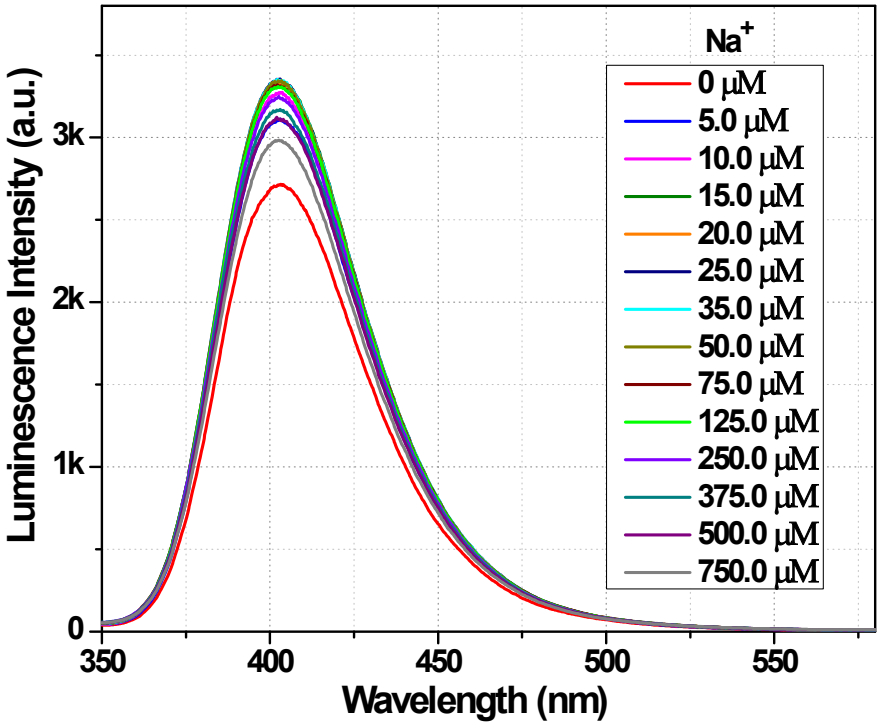

Fig. S20 Emission spectra of **1** dispersed in water upon incremental addition of Na^+ solution (λ_{ex} = 300 nm). The final concentration of Na^+ in the medium is indicated in the legend.

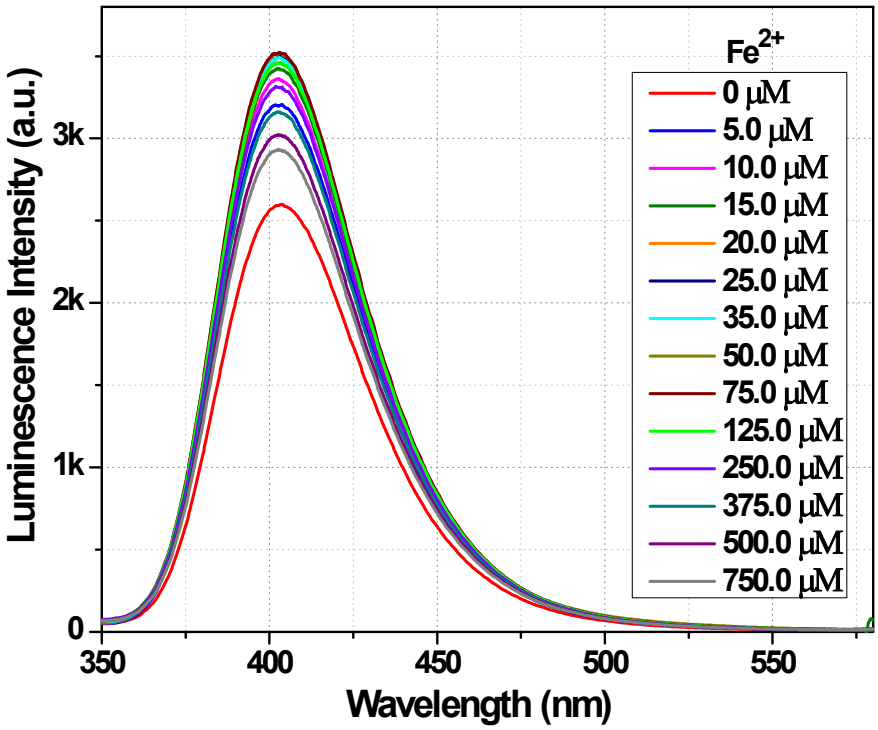

Fig. S21 Emission spectra of **1** dispersed in water upon incremental addition of Fe^{2+} solution (λ_{ex} = 300 nm). The final concentration of Fe^{2+} in the medium is indicated in the legend.

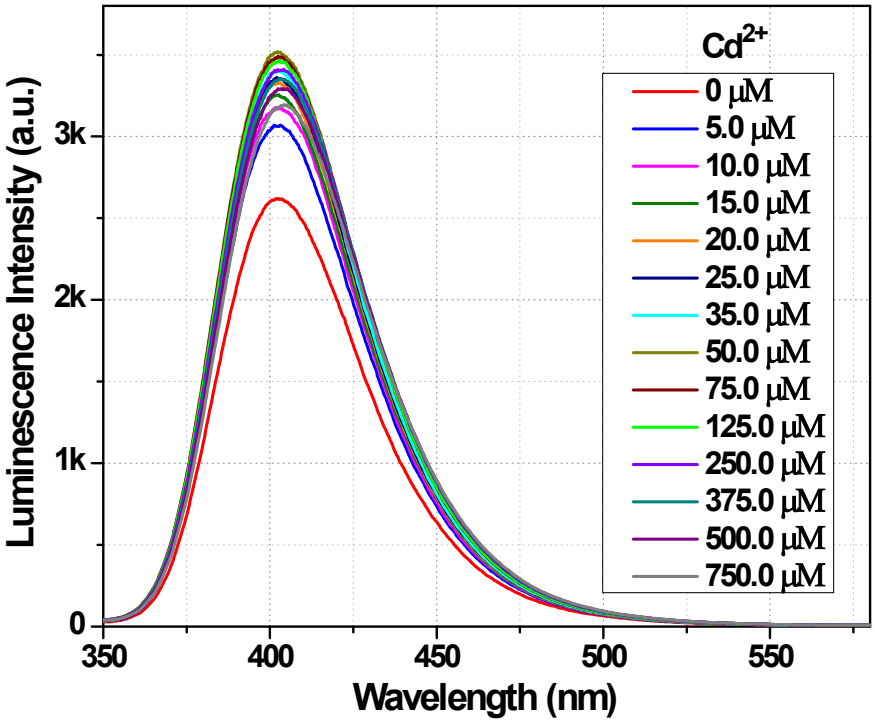

Fig. S22 Emission spectra of **1** dispersed in water upon incremental addition of Cd^{2+} solution (λ_{ex} = 300 nm). The final concentration of Cd^{2+} in the medium is indicated in the legend.

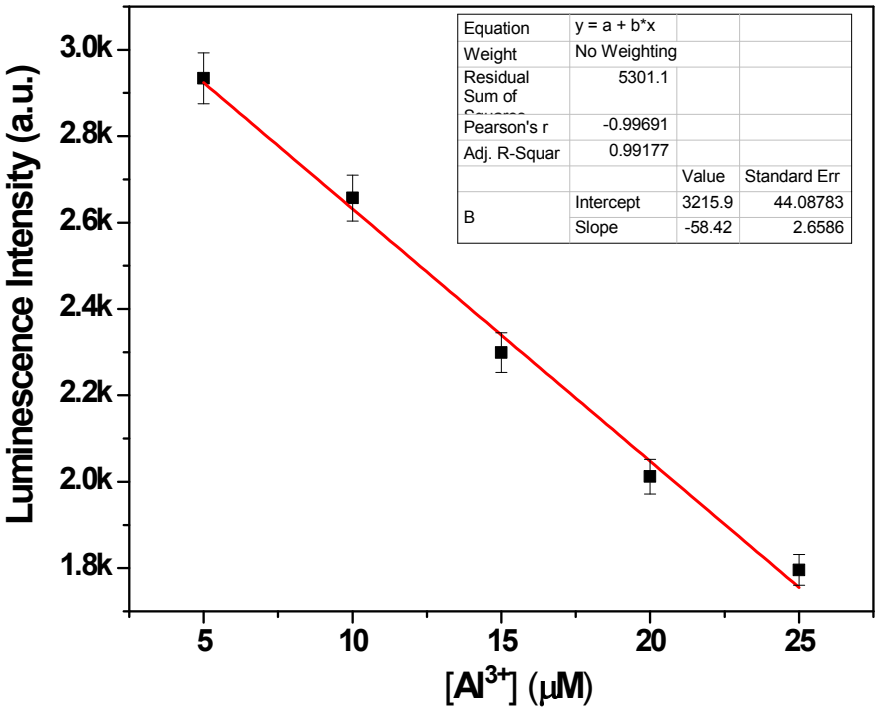

Fig. S23 The plot of the luminescence intensity of **1** as a function of concentration of Al^{3+} ion. The black square points represent the data points with error bars from experiment and the red line is the linear fitted line to the data points.

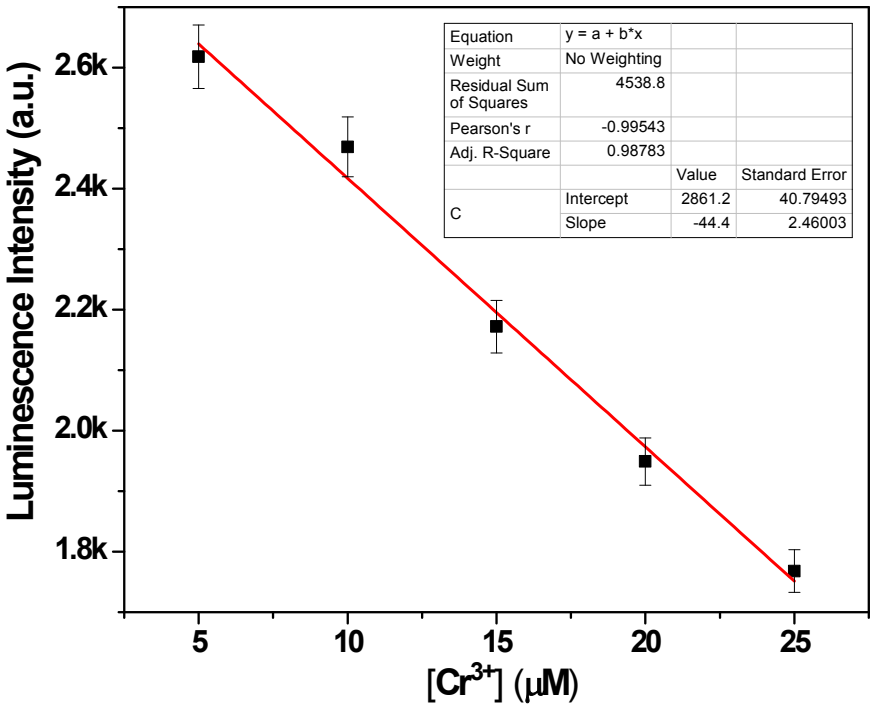

Fig. S24 The plot of the luminescence intensity of **1** as a function of concentration of Cr^{3+} ion. The black square points represent the data points with error bars from experiment and the red line is the linear fitted line to the data points.

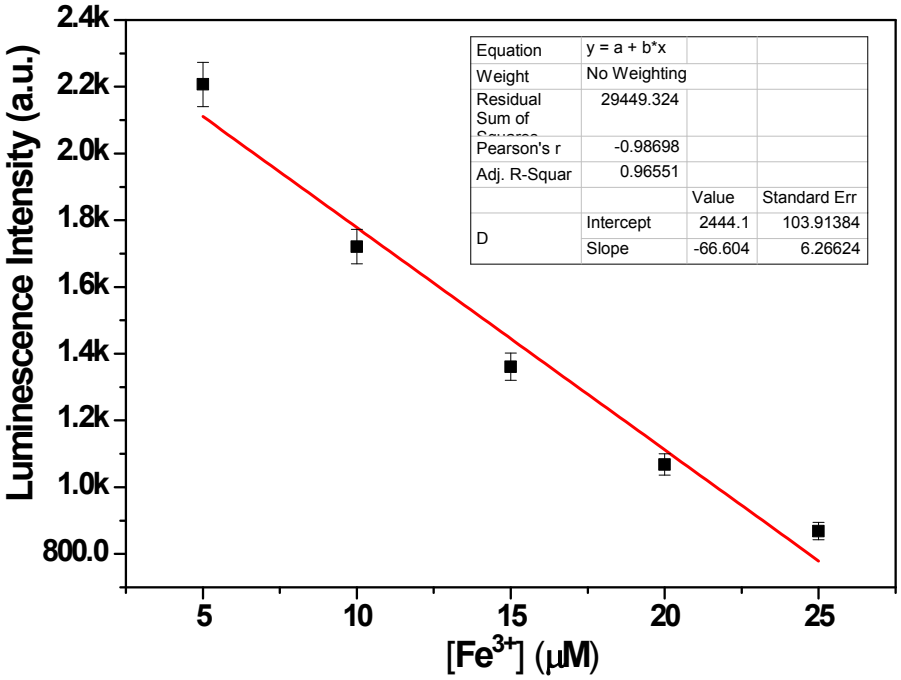

Fig. S25 The plot of the luminescence intensity of **1** as a function of concentration of Fe^{3+} ion. The black square points represent the data points with error bars from experiment and the red line is the linear fitted line to the data points.

Table S3. Calculation of Standard Deviation and Limit of Detection (LOD) for Al^{3+}, Cr^{3+} and Fe^{3+}:

Blank Reading (only **1**)	Fluorescence Intensities at 421 nm (X)	Mean (x)	Standard Deviation $(\sigma) = \sqrt{\frac{\sum \lvert X - x \rvert^2}{N}}$
Reading 1	3545	3534.2	6.852
Reading 2	3527		
Reading 3	3528		
Reading 4	3532		
Reading 5	3539		

Slope, m for Al^{3+} = 58.42

Slope, m for Cr^{3+} = 44.40

Slope, m for Fe^{3+} = 66.60

LOD for Al^{3+} = $3\sigma/m$ = (3 × 6.852)/58.42 = 0.35 μM = 8.43 ppb

By repeating the experiment 3 times, the uncertainty have been calculated to be ± 0.007. So, the LOD value for Al^{3+} = 0.35 ± 0.007 μM.

LOD for Cr^{3+} = $3\sigma/m$ = (3 × 6.852)/44.40 = 0.46 μM = 22.63 ppb

By repeating the experiment 3 times, the uncertainty have been calculated to be ± 0.009. So, the LOD value for Cr^{3+} = 0.46 ± 0.009 μM.

LOD for Fe^{3+} = $3\sigma/m$ = (3 × 6.852)/66.60 = 0.30 μM = 15.85 ppb

By repeating the experiment 3 times, the uncertainty have been calculated to be ± 0.006. So, the LOD value for Fe^{3+} = 0.30 ± 0.006 μM.

where, σ is the standard deviation and m is the slope of the plot of luminescence intensity *vs.* concentration of analyte.

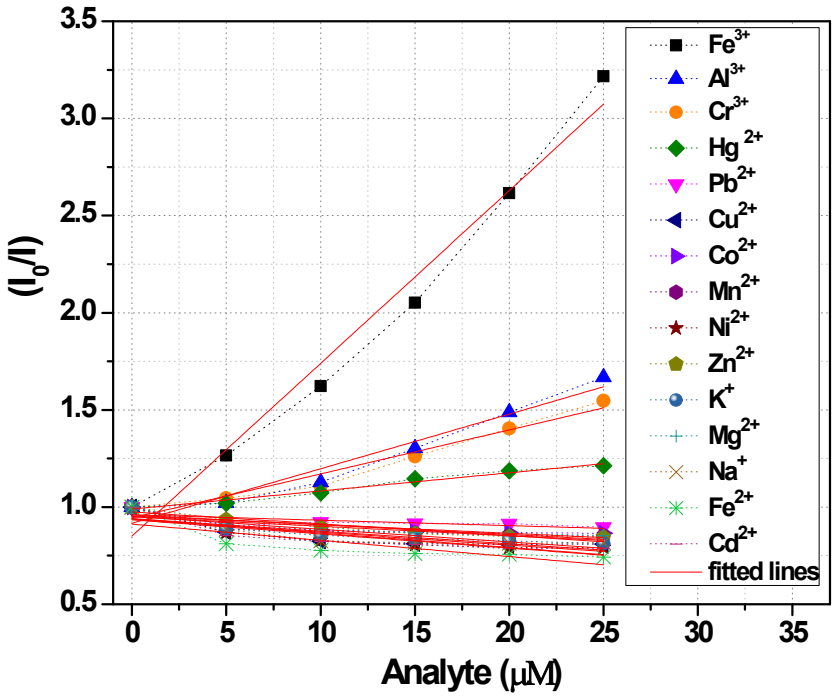

Fig. S26 The plot of (I_0/I) of **1** (at 403 nm) *vs.* concentration of analytes, [C] (up to 25 μM). I_0 and I are the luminescence intensities of **1** in the absence and presence of the analyte, respectively. The solid red lines represent the linear fits to the data.

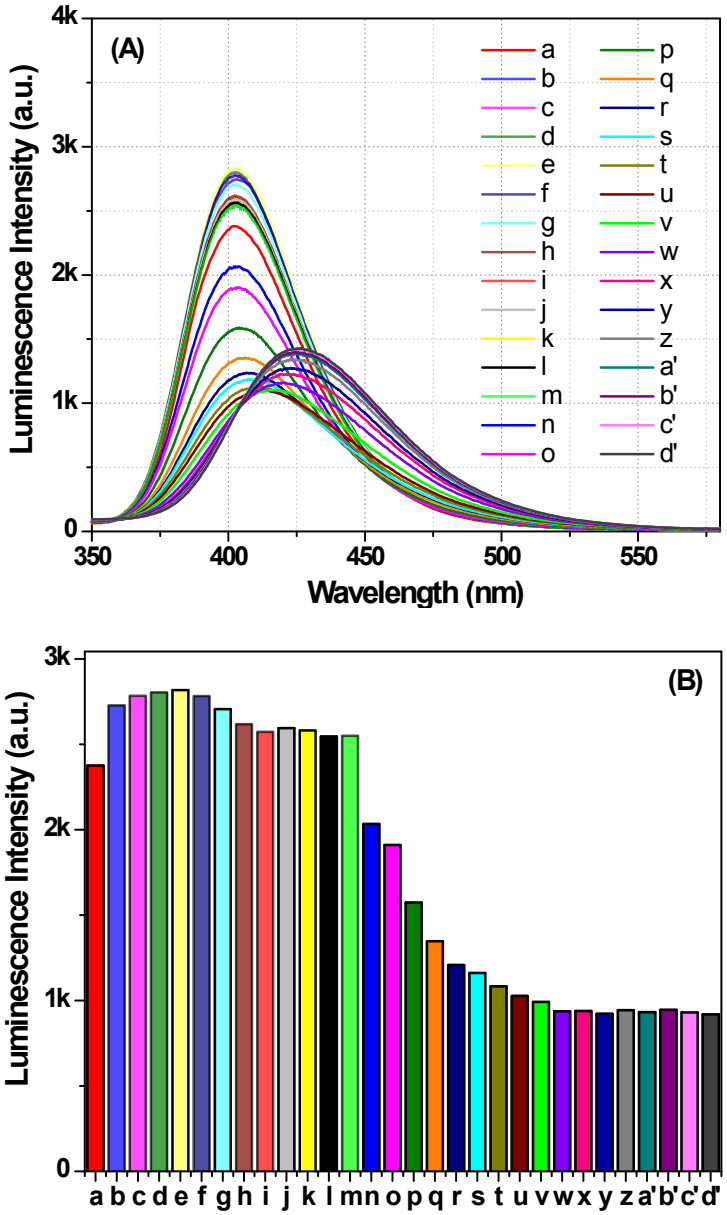

Fig. S27 (A) Emission spectra of **1** dispersed in aqueous solution upon the cumulative addition of different metal ions followed by stepwise addition of Al^{3+} ion (λ_{ex} = 300 nm). (B) Bar diagram showing the luminescence intensity (monitored at 403 nm) after the sequential addition of the other metal ions and Al^{3+} ion. The composition and concentration of the system were as follows: (a) **1** in aqueous solution, (b) a + 15 μM Mg^{2+}, (c) b + 15 μM K^{+}, (d) c + 15 μM Ni^{2+}, (e) d + 15 μM Na^{+}, (f) e + 15 μM Cu^{2+}, (g) f + 15 μM Hg^{2+}, (h) g + 15 μM Pb^{2+}, (i) h + 15 μM Fe^{2+}, (j) i + 15 μM Cd^{2+}, (k) j + 15 μM Zn^{2+}, (l) k + 15μM Co^{2+} (m) l + 15 μM Mn^{2+}, (n) m + 10 μM Al^{3+}, (o) m + 15 μM Al^{3+}, (p) m + 25 μM Al^{3+}, (q) m + 35 μM Al^{3+}, (r) m + 45 μM Al^{3+}, (s) m + 50 μM Al^{3+}, (t) m + 62.5 μM Al^{3+}, (u) m + 75 μM Al^{3+}, (v) m + 100 μM Al^{3+}, (w) m + 150 μM Al^{3+}, (x) m + 200 μM Al^{3+}, (y) m + 250 μM Al^{3+}, (z) n + 350 μM Al^{3+}, (a′) n + 450 μM Al^{3+} and (b′) n + 500 μM Al^{3+} (c′) n + 625 μM Al^{3+} (d′) n + 750 μM Al^{3+}.

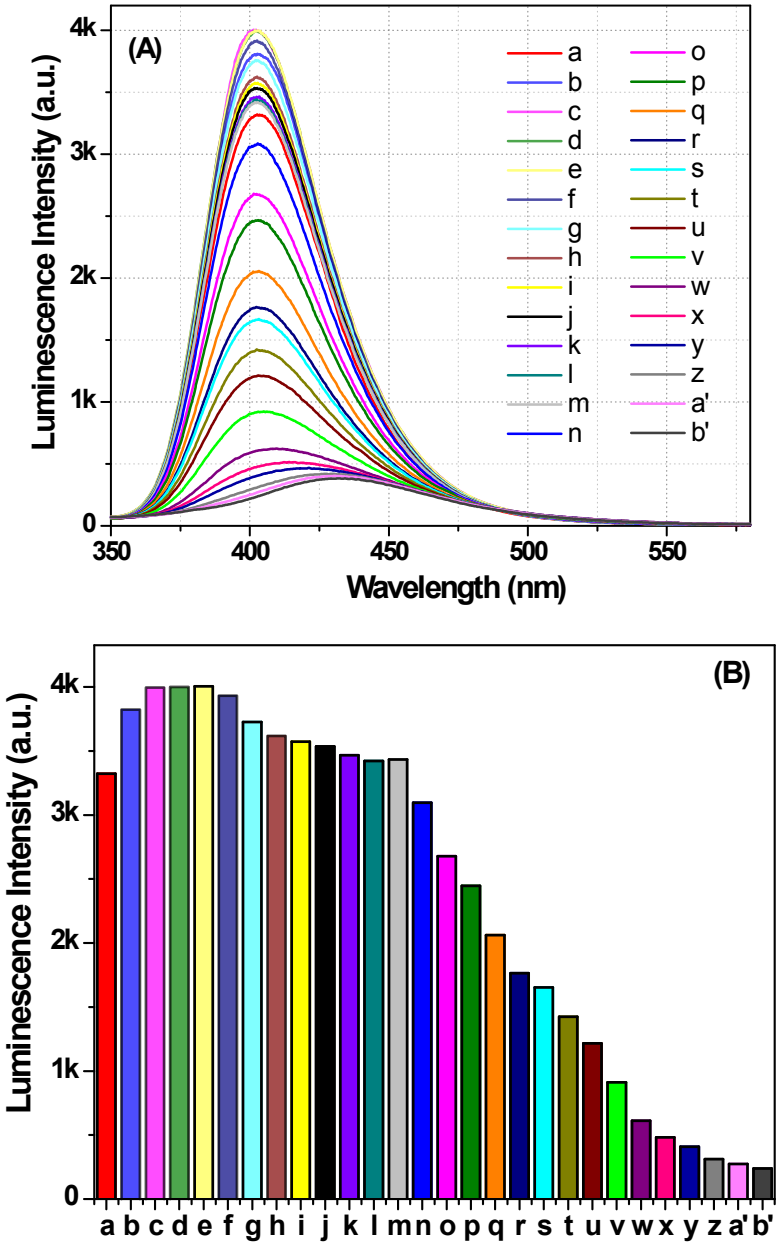

Fig. S28 (A) Emission spectra of **1** dispersed in aqueous solution upon the cumulative addition of different metal ions followed by stepwise addition of Cr^{3+} ion (λ_{ex} = 300 nm). (B) Bar diagram showing the luminescence intensity (monitored at 403 nm) after the sequential addition of the other metal ions and Cr^{3+} ion. The composition and concentration of the system were as follows: (a) **1** in aqueous solution, (b) a + 15 μM Mg^{2+}, (c) b + 15 μM K^{+}, (d) c + 15 μM Ni^{2+}, (e) d + 15 μM Na^{+}, (f) e + 15 μM Cu^{2+}, (g) f + 15 μM Hg^{2+}, (h) g + 15 μM Pb^{2+}, (i) h + 15 μM Fe^{2+}, (j) i + 15 μM Cd^{2+}, (k) j + 15 μM Zn^{2+}, (l) k + 15μM Co^{2+} (m) l + 15 μM Mn^{2+}, (n) m + 10 μM Cr^{3+}, (o) m + 20 μM Cr^{3+}, (p) m + 25 μM Cr^{3+}, (q) m + 35 μM Cr^{3+}, (r) m + 45 μM Cr^{3+}, (s) m + 50 μM Cr^{3+}, (t) m + 62.5 μM Cr^{3+}, (u) m + 75 μM Cr^{3+}, (v) m + 100 μM Cr^{3+}, (w) m + 150 μM Cr^{3+}, (x) m + 200 μM Cr^{3+}, (y) m + 250 μM Cr^{3+}, (z) m + 375 μM Cr^{3+}, (a□) m + 500 μM Cr^{3+} and (b□) m + 750 μM Cr^{3+}.

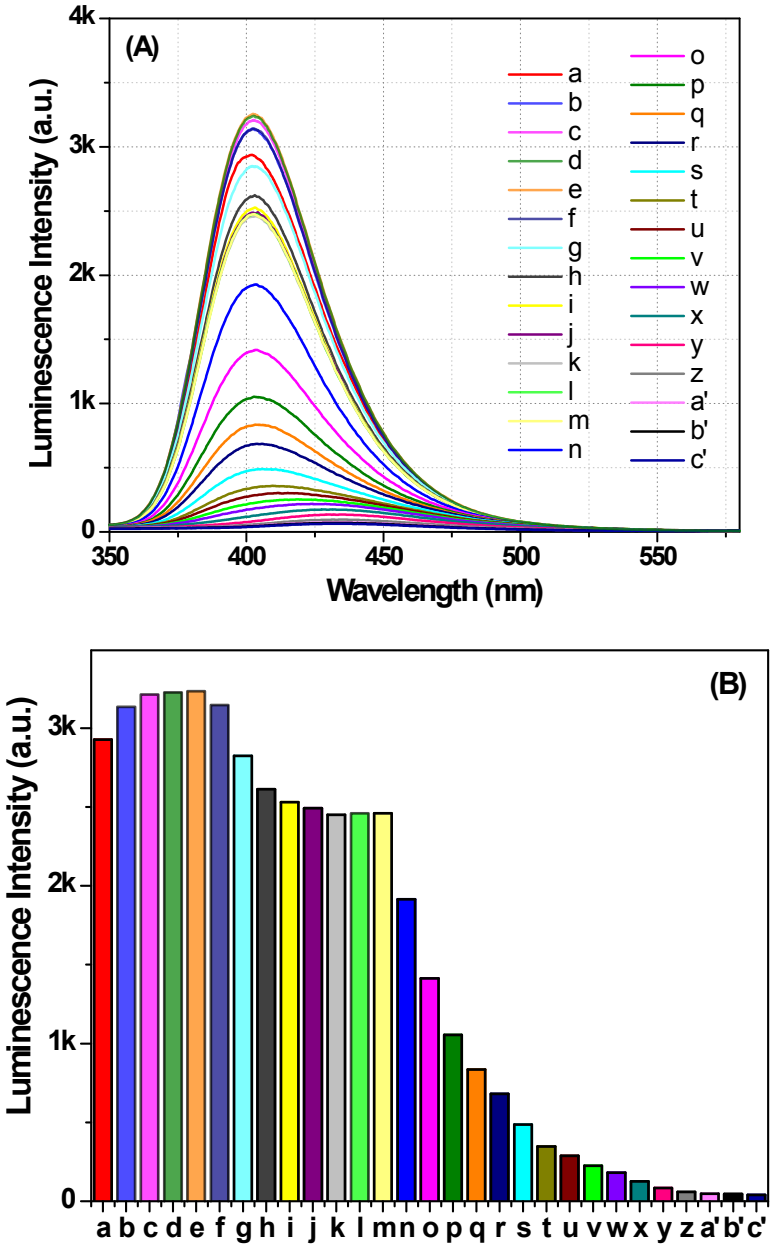

Fig. S29 (A) Emission spectra of **1** dispersed in aqueous solution upon the cumulative addition of different metal ions followed by stepwise addition of Fe^{3+} ion (λ_{ex} = 300 nm). (B) Bar diagram showing the luminescence intensity (monitored at 403 nm) after the sequential addition of the other metal ions and Fe^{3+} ion. The composition and concentration of the system were as follows: (a) **1** in aqueous solution, (b) a + 15 μM Mg^{2+}, (c) b + 15 μM K^{+}, (d) c + 15 μM Ni^{2+}, (e) d + 15 μM Na^{+}, (f) e + 15 μM Cu^{2+}, (g) f + 15 μM Hg^{2+}, (h) g + 15 μM Pb^{2+}, (i) h + 15 μM Fe^{2+}, (j) i + 15 μM Cd^{2+}, (k) j + 15 μM Zn^{2+}, (l) k + 15μM Co^{2+} (m) l + 15 μM Mn^{2+}, (n) m + 5 μM Fe^{3+}, (o) m + 10 μM Fe^{3+}, (p) m + 15 μM Fe^{3+}, (q) m + 20 μM Fe^{3+}, (r) m + 25 μM Fe^{3+}, (s) m + 35 μM Fe^{3+}, (t) m + 45 μM Fe^{3+}, (u) m + 50 μM Fe^{3+}, (v) m + 62.5 μM Fe^{3+}, (w) m + 75 μM Fe^{3+}, (x) m + 100 μM Fe^{3+}, (y) m + 150 μM Fe^{3+}, (z) m + 200 μM Fe^{3+}, (a□) m + 250 μM Fe^{3+}, (b□) m + 500 μM Fe^{3+} and (c□) m + 750 μM Fe^{3+}.

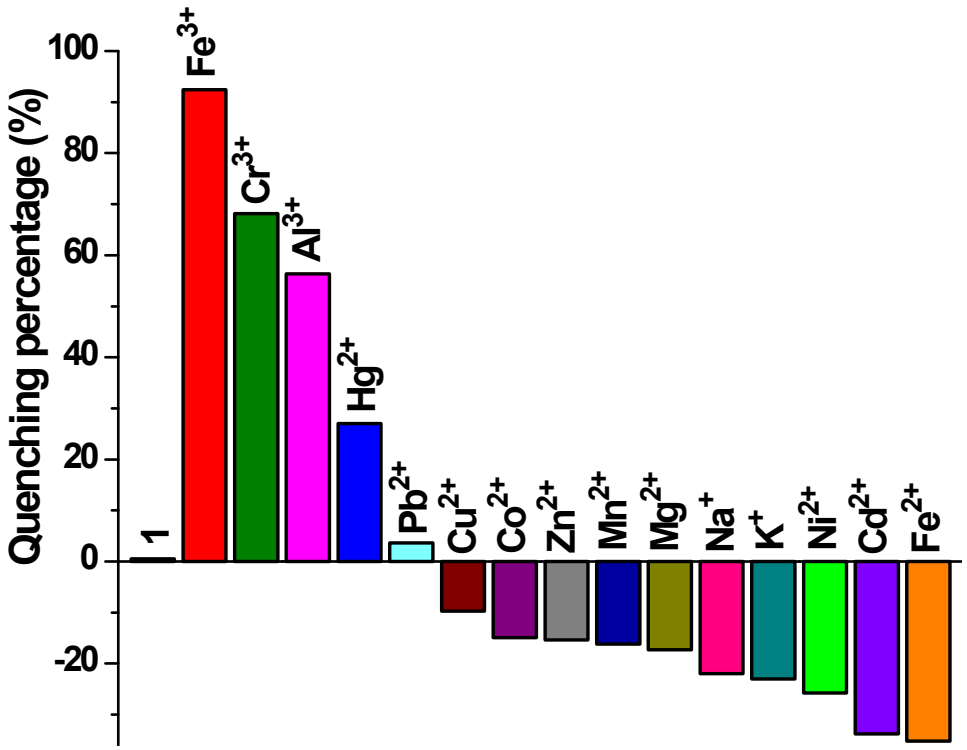

Fig. S30 Quenching percentage (monitored at 403 nm) with respect to the emission of an aqueous suspension of **1** after the addition of 75 μM of different metal ions.

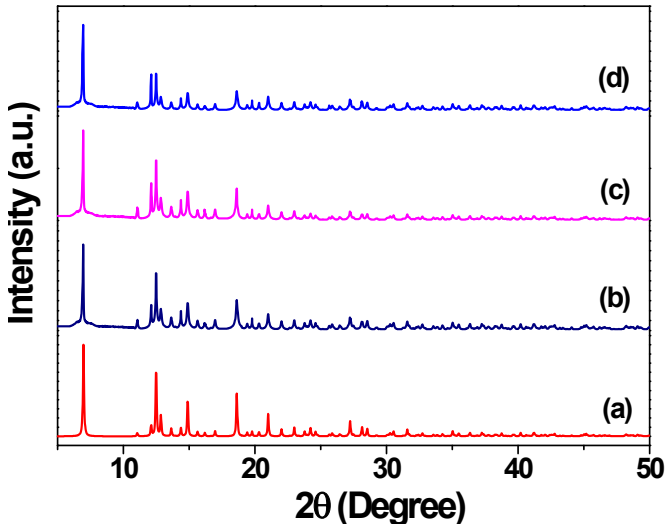

Fig. S31 The PXRD pattern of **1**: (a) simulated from single-crystal X-ray data, (b) immersed in an aqueous solution of Al^{3+}, (c) immersed in an aqueous solution of Cr^{3+} and (d) immersed in an aqueous solution of Fe^{3+}.

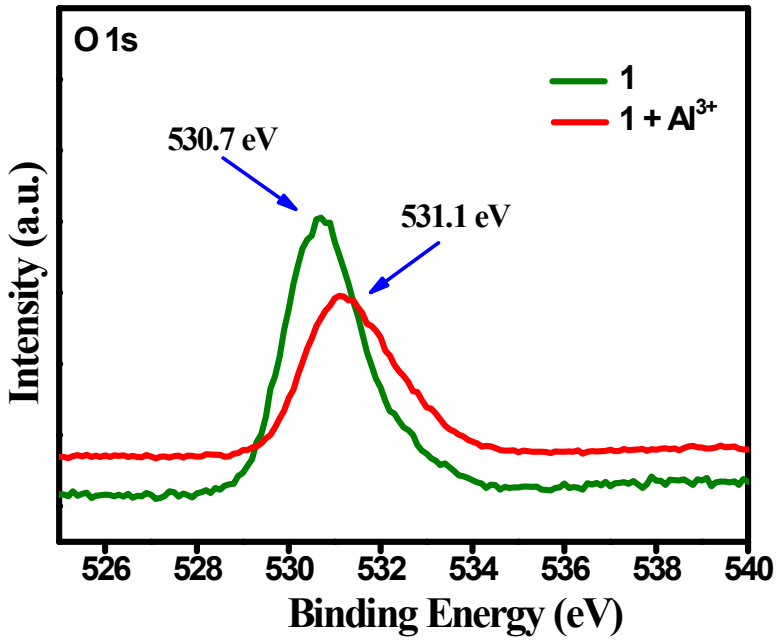

Fig. S32 O 1s XPS spectra of **1** before and after the addition of Al^{3+}.

XPS measurements was performed before and addition of Al^{3+}. The XPS method revealed that the O 1s from the oxygen atom at 530.7 eV attributed to the carboxylate group in the aromatic ring in **1** is shifted to 531.1 eV in the presence of Al^{3+} . This shift and higher binding energy of the O 1s of **1** immersed in Al^{3+} compared to **1** clearly confirms that there exists a strong coordination environment between the oxygen atom of the carboxylate group and the Al^{3+} ion.

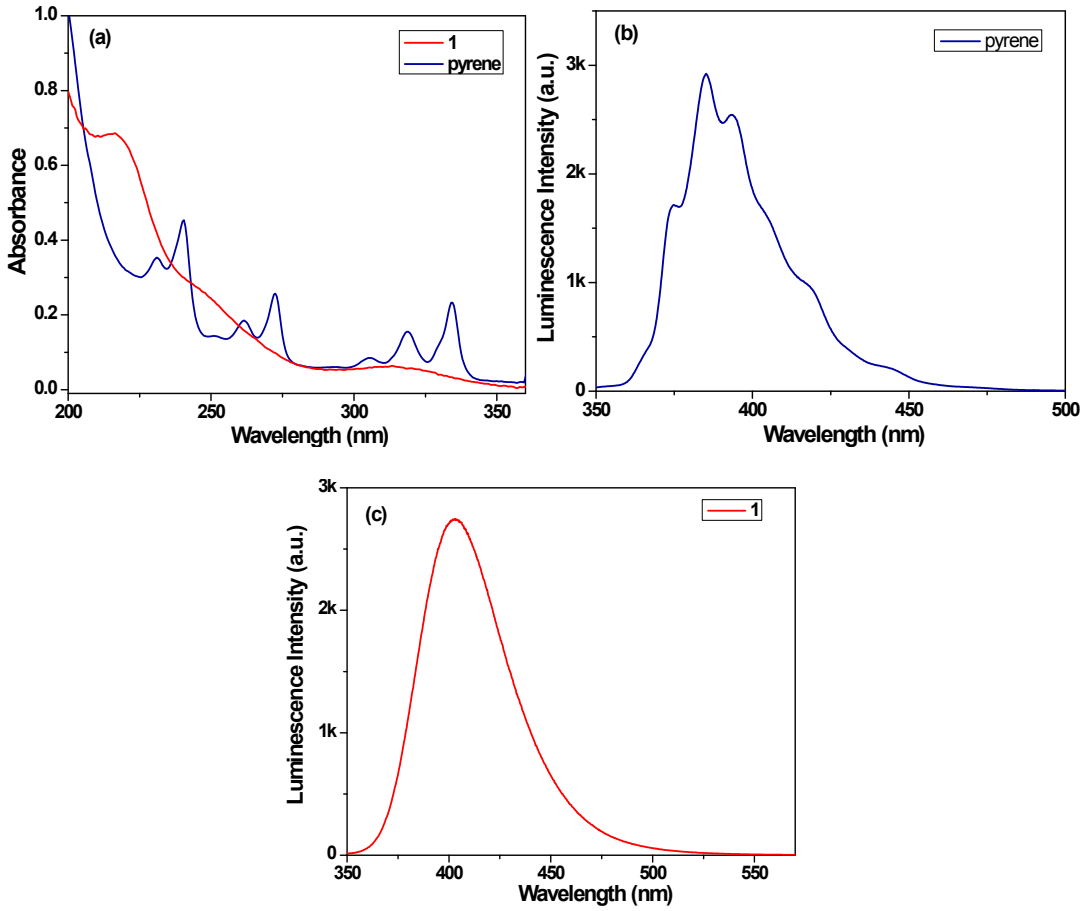

Fig. S33 (a) Absorption spectra of **1** in an aqueous suspension and pyrene in heptane, (b) luminescence spectra of pyrene upon excitation at 300 nm, and (c) luminescence spectra of **1** upon excitation at 300 nm.

Determination of quantum yield:

where Q_f^i and Q_f^s are the fluorescence QYs of the sample and that of the standard, respectively; F^i and F^s are the integrated intensities (areas) of sample and standard spectra, respectively; $f_s and\, f_i$ are the absorbance factor of standard and sample, respectively; the refractive indices of the sample and reference solution are n_i and n_s, respectively.

$$\phi_f^i = \frac{152712 \times 0.0629 \times 1.33^2}{108303 \times 0.0544 \times 1.38^2} \times 0.3$$

$$\phi_f^i = 0.45$$